

Optimization of x-ray units with CDRAD phantom: can it predict the radiologist opinion?

Poster No.: C-1619
Congress: ECR 2013
Type: Scientific Exhibit
Authors: R. G. L. Decoster, H. Mol; Brussels/BE
Keywords: Radiation safety, Diagnostic procedure, Conventional radiography, Radioprotection / Radiation dose, Radiation physics, Musculoskeletal system, Cost-effectiveness, Image verification
DOI: 10.1594/ecr2013/C-1619

Any information contained in this pdf file is automatically generated from digital material submitted to EPOS by third parties in the form of scientific presentations. References to any names, marks, products, or services of third parties or hypertext links to third-party sites or information are provided solely as a convenience to you and do not in any way constitute or imply ECR's endorsement, sponsorship or recommendation of the third party, information, product or service. ECR is not responsible for the content of these pages and does not make any representations regarding the content or accuracy of material in this file.

As per copyright regulations, any unauthorised use of the material or parts thereof as well as commercial reproduction or multiple distribution by any traditional or electronically based reproduction/publication method ist strictly prohibited.

You agree to defend, indemnify, and hold ECR harmless from and against any and all claims, damages, costs, and expenses, including attorneys' fees, arising from or related to your use of these pages.

Please note: Links to movies, ppt slideshows and any other multimedia files are not available in the pdf version of presentations.

www.myESR.org

Purpose

In film-screen radiography, the density depends on a correct exposure and processing of the film. This result is a permanent record and it cannot be manipulated. (1) Transition to digital detectors was a major innovation for medical imaging departments. (1-6) The fixed correlation between film density and detector-air-kerma (DAK) has vanished in the digital world. (1,4,7) The larger dynamic range tolerates a wider DAK range without an adverse effect on the image quality. Higher DAK's do not only lower the noise levels in the radiography, they also deliver a crisp and sharp appearance, which is favoured by the radiologist. (4,7) The wide dynamic range offers the possibility to further 'tailor' the patient dose and image quality for a specific task. (4,8) This paradigm shift demands new guidelines and illustrates the challenge for practitioners to regain control over the relation between dose and image quality. (4,9)

Not many authors tried to define the concept of image quality, notwithstanding the widespread use of the term. (10,11) The image quality needed is closely related to the clinical question, as not all imaging tasks demand the same diagnostic information. These differences illustrate the relation between the diagnostic task ahead and the published dose reductions. (1,4,11-13) The possibility to detect pathological structures correlates to the reproduction of normal anatomy. (10,14) Therefore well-defined clinical image quality criteria are needed for a given type of examination. (9,10,12,14,15)

If one could predict this detectability one could optimize x-ray units without the exposure of patients. Many radiology departments need such an optimization procedure, what accentuates the need for a cost-effective solution. Objective image quality measurements (DQE, NNPS, SNR) are often technically complex and difficult to implement on a routine basis. Furthermore, they don't include the effect of scatter radiation or the influence of specific characteristics of the observer. (6,16,17)

The CDRAD phantom, developed for the quantification and psychophysical evaluation of image detectors, could be a cost-effective alternative. (6,16) Due to the lack of anatomical noise the CDRAD phantom can't directly predict the clinical image quality. (5,16) But it provides useful information on the contrast detail detectability and allows comparing the visualisation of low-contrast structures (fissures in bony structures) among different x-ray units. (5,16,18)

The purpose of this study is to evaluate the ability of the CDRAD phantom to predict the systems ability visualize anatomic structures. General differences between Computed Radiography (CR) and Digital Radiography (DR) are expected as evidence shows that even at the lowest DAK DR provides a better CDRAD and IQFInv. The question remains if CDRAD can predict the visibility between different CR and DR systems. (5,6,13,16)

Methods and Materials

To assess the image quality 168 anterior-posterior (AP) radiographs of the knee were collected in 17 radiology centres across Flanders. The radiographs were anonymized and stored on optical carriers. Next to the radiograph, additional information on positioning, patient's morphology and technique were recorded. Subgroups are defined based on detector technology: CR and DR. An absolute Visual Grading Analysis (VGA) was used to judge and quantify the visibility of different anatomic structures. (14,19,20) The anatomic structures to evaluate were collected from the guidelines published by the European Commission, radiography textbooks and different publications with a similar purpose. (10,14,21-23) Moreover, five radiologists reviewed the 2 sets of criteria during structured interviews until saturation. (Table 1)

Table 1: Criteria for the evaluation of the radiographs

Knee AP	Pelvis AP
<ul style="list-style-type: none">• Visualization of the patella• Visually sharp reproduction of the tibial plateau• Visually sharp reproduction of the intercondylar eminence and fossa• Visually sharp reproduction of the femoral condyles• Visually sharp reproduction of the caput fibulae• Transition of cortical to trabecular bone	<ul style="list-style-type: none">• Visualization of sacroiliac joints• Visualization of the middle third of the iliac crest• Visualization of the pubic and ischial rami• Visually sharp reproduction of the collum femoris• Visually sharp reproduction of the trochanters• Visually sharp reproduction of the Shenton's line

Subsequently, six experienced radiologists scored both datasets with ViewDex[®] (Version 2.0) on a five-point scale (from 1 'bad' to 5 'excellent') where the mid-point was equalized to diagnostic image quality or the image quality that would be expected routinely when imaging cooperative patients. (11,14,19,20) All observations took place in a controlled environment on a standard workstation (Windows7-64bit) equipped with a Barco's[®] Corionis display and Barco[®] QAWeb. The display operated within the boundaries of the AAPM TG18. Options such as window/level, pan and zoom were available. (4,26) Prior to the VGA, each observer received a training dataset. Moreover, twenty radiographs were repeated during the VGA to determine intra-observer variability. Results from the training dataset were discarded.

For each image, a VGA score (VGAS) was calculated using following equation:

$$VGA = \frac{\sum_{i=1}^I \sum_{s=1}^S \sum_{o=1}^O G_{i,s,o}}{I \times S \times O}$$

Fig. 1

References: Medical Imaging, PRAGODI - Centre for Practice-based Research and Services, HUBrussel - Brussels/BE

where $G_{i,s,o}$ is the grading for image i , structure s and observer o . The denominator is formed by I , the total number of images, S for the number of evaluated structures and O the number of observers in the study. (27) This numeric expression, the Visual Grading Analysis Score (VGAS), defines the mean score over all observations. (14) Hereby the VGAS can serve as an indicator for the image quality as appreciated by the radiologists.

A CDRAD phantom (University Medical Center Nijmegen, Nijmegen, The Netherlands) was used to quantify the image quality, independent of the diagnostic question and characteristics of the radiologists. (5,6) The CDRAD is polymethylmethacrylate (PMMA) plate divided in a matrix of 15x15-squared cells containing logarithmically varied holes in depth and diameter. (18,29) To simulate the object thickness and absorption the CDRAD was enveloped with 15cm of PMMA. (16) In order to quantify the image quality eight radiographs for each x-ray unit were produced with the same clinical protocol used to produce the collected images. The radiographs were processed with a flat field algorithm and a speed class according to the clinical program. The radiographs were processed with the CDRAD Analyser (version 12.1.12, Artinis Medical Systems B.V.) (5,16) The analyzer delivered a CDCurve and IQFInv. (13)

Statistical analyses of the VGAS and IQFInv between groups were performed with a one-way ANOVA followed by post hoc tests with Bonferroni correction using SPSS 19.0. A p -value < 0.05 denotes a significant difference between two data points. To analyse intra-observer variability a Pearson correlation test is used. The inter-observer variability is investigated with a non-parametric, rank-invariant Spearman correlation. The relation between the VGAS and the general appreciation of the radiography is investigated with a Paired-Samples T-test. Correlation between IQFInv, VGAS and DAK are assessed with the Spearman correlation. The Detector Air Kerma (DAK) was specified for each included x-ray unit using the Signal Transfer Properties (STP) of the detector. These calculations were performed conform the protocol defined by the IPEM. (28)

Results

3. Results

The complete dataset for the knee AP was analysed by six radiologists with a minimum of five year reporting experience in judging digital radiographs. Subgroups of radiographs, based on detector technology, are comparable in composition: a similar distribution in sex and no significant BMI was noted. For the other factors (Table 2) a significant difference ($p < 0.01$) is observed.

Table 2: Results for the knee AP

	N	Sex		BMI	Tube Voltage [kV]	Tube Load [mAs]	FRA [cm]	DAK [μ Gy]	VGAS	IQFInv
		Male	Female							
CR	96	48	48	25.65 ± 4.8	69.63 ± 4.8	30.39 ± 62	103.44 ± 5.95	4.08 \pm 1.47	3.82 \pm 0.38	3.72 \pm 0.63
DR	72	38	34	25.73 ± 3.45	64.28 ± 2.58	8.82 \pm 3.97	115.16 ± 4.5	2.99 \pm 2.14	4.07 \pm 0.32	4.98 ± 0.75
Total	168	86	82	25.68 ± 4.23	67.33 ± 4.79	20.56 ± 47	108.46 ± 7.92	3.63 \pm 1.85	3.91 \pm 0.39	4.27 \pm 0.93

The anterior-posterior radiograph of the knee obtained an average VGAS of 3.91 and an average IQFInv of 4.27. A significant ($p < 0.01$) difference between CR and DR was noted. The difference in IQFInv is also graphically demonstrated in the CDCurves. (Figure 2)

According to the Spearman's Rho, scores of each observer correlated strongly and significant ($p < 0.01$) with the total VGAS-score. Only 1 observer had a rather weak, but still significant at the 0.01 significance level, correlation (0.394) between her general appreciation of each image and the VGAS of the images. The intra-observer variability was not significant. No significant correlation between the DAK and the VGAS was found, nor for CR (-0.005; $p = 0.985$; 1.61 μ Gy-5.48 μ Gy) or DR (-0.109; $p = 0.365$; 0.43 μ Gy-6.18 μ Gy). Neither was there a significant correlation between VGAS and IQFInv for CR (0.137; $p = 0.189$) or for DR (-0.149; $p = 0.215$). A strong, significant negative correlation (-0.780; $p < 0.01$) was present between DAK and IQFInv for CR. In DR this correlation (0.339; $p < 0.05$) was weak but significant. A possible origin of the difference is graphically demonstrate by the CDCurve and lies in the zone of the lower contrasts. (Figure 3-4)

Images for this section:

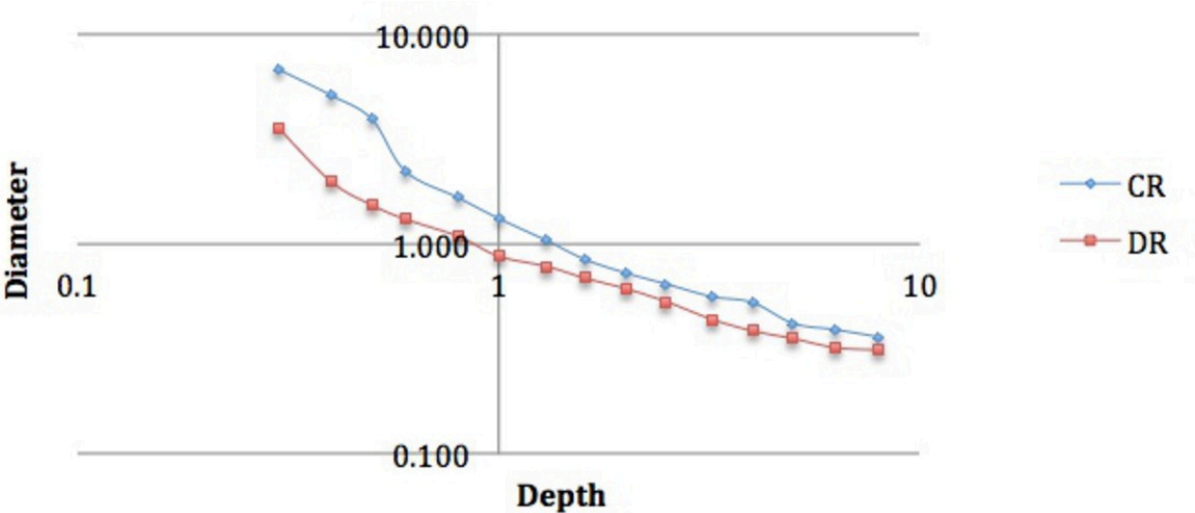


Fig. 2: CDCurve of the CR and DR subgroups for the knee AP

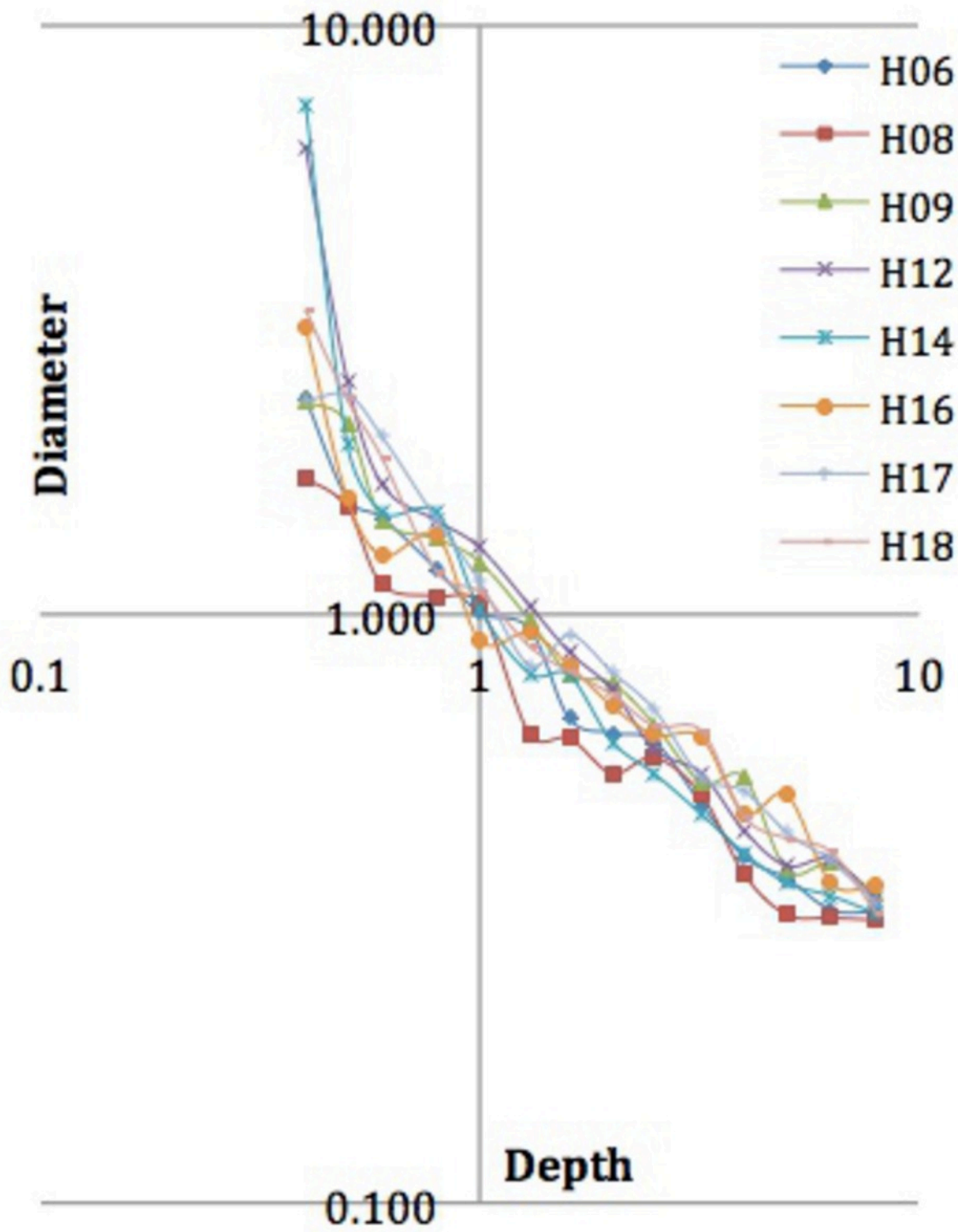


Fig. 3: CDCurve of the diferente DR untis

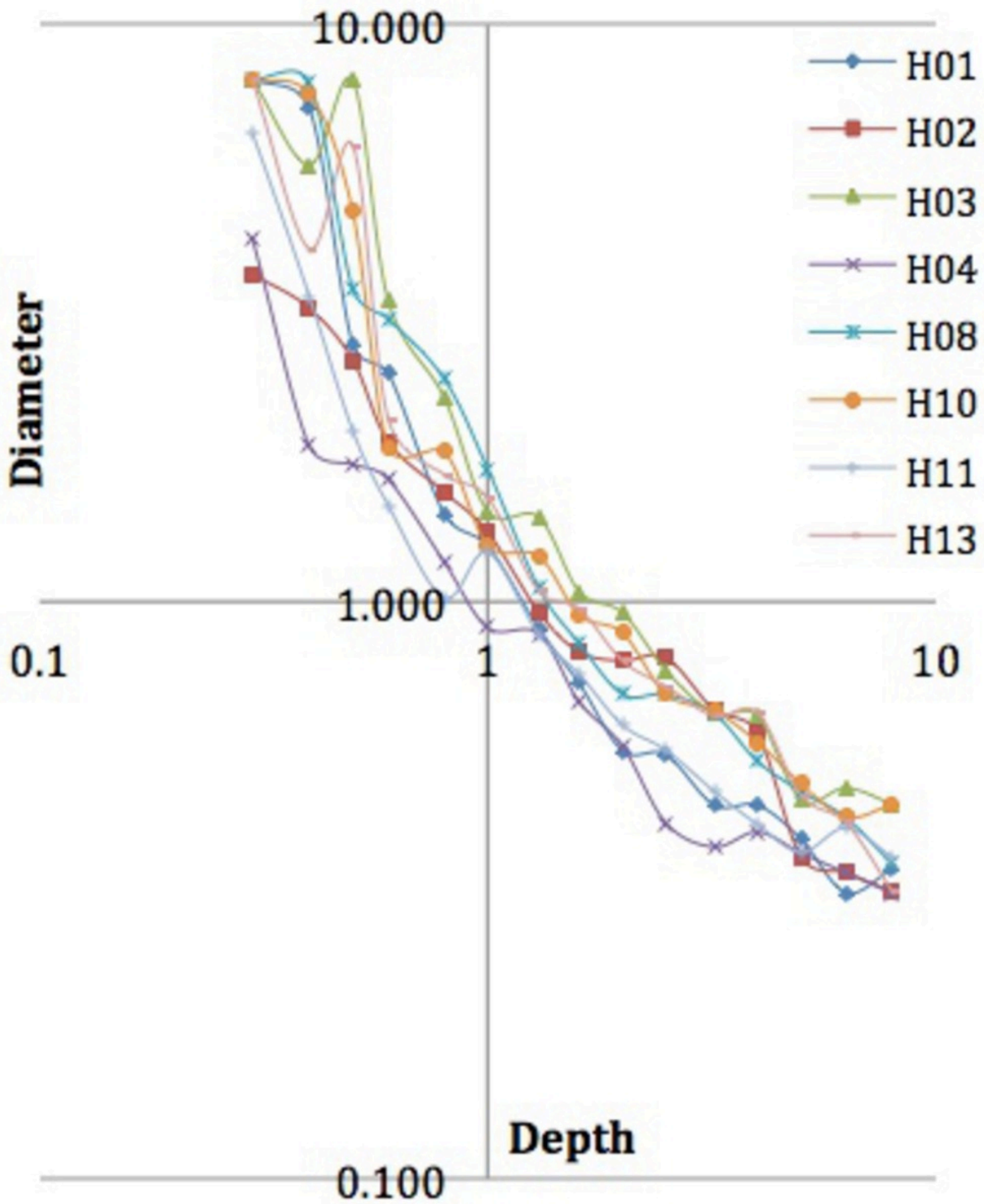


Fig. 4: CDCurve of the diferente CR units

Conclusion

As expected, a significant difference in VGAS rated image quality between the CR and DR was noted. The VGA revealed an image quality higher than diagnostic necessary in both datasets with a high correlation between observers. No correlations supporting the hypothesis of predicting the appreciation with CDRAD were found in this dataset. These results substantiate the argument that in this dataset the relation between DAK and image quality is non-existent.

References

1. Busch HP, Faulkner K. Image quality and dose management in digital radiography: A new paradigm for optimisation. *Radiat Prot Dosimetry* 2005;117(1-3):143-7.
2. Lança L, Silva A. Digital radiography detectors-a technical overview: Part 1. *Radiography* 2009;15(1):58-62.
3. Lança L, Silva A. Digital radiography detectors-a technical overview: Part 2. *Radiography* 2009;15(2):134-8.
4. ICRP. Managing patient dose in digital radiology. A report of the international commission on radiological protection. *Ann ICRP* 2004;34(1):1-73.
5. Veldkamp WJ, Kroft LJ, Boot MV, Mertens BJ, Geleijns J. Contrast-detail evaluation and dose assessment of eight digital chest radiography systems in clinical practice. *Eur Radiol* 2006, Feb;16(2):333-41.
6. Peer S, Neitzel U, Giacomuzzi SM, Peer R, Gassner E, Steingruber I, Jaschke W. Comparison of low-contrast detail perception on storage phosphor radiographs and digital flat panel detector images. *IEEE Trans Med Imaging* 2001, Mar;20(3):239-42.
7. Willis CE, Slovis TL. The ALARA concept in pediatric CR and DR: Dose reduction in pediatric radiographic exams--a white paper conference. *AJR Am J Roentgenol* 2005, Feb;184(2):373-4.
8. Völk M, Hamer OW, Feuerbach S, Strotzer M. Dose reduction in skeletal and chest radiography using a large-area flat-panel detector based on amorphous silicon and thallium-doped cesium iodide: Technical background, basic image quality parameters, and review of the literature. *Eur Radiol* 2004, May;14(5):827-34.
9. Faulkner K. The DIMOND project and its impact on radiation protection. *Radiat Prot Dosimetry* 2005;117(1-3):3-6.
10. Sund P, Båth M, Kheddache S, Månsson LG. Comparison of visual grading analysis and determination of detective quantum efficiency for evaluating system performance in digital chest radiography. *Eur Radiol* 2004;14(1):48-58.

11. Shet N, Chen J, Siegel EL. Continuing challenges in defining image quality. *Pediatr Radiol* 2011, May;41(5):582-7.
12. Moores BM, Mattsson S, Månsson LG, Panzer W, Regulla D, Dance D, et al. RADIUS--closing the circle on the assessment of imaging performance. *Radiat Prot Dosimetry* 2005;114(1-3):450-7.
13. Fischbach F, Ricke J, Freund T, Werk M, Spors B, Baumann C, et al. Flat panel digital radiography compared with storage phosphor computed radiography: Assessment of dose versus image quality in phantom studies. *Invest Radiol* 2002, Nov;37(11):609-14.
14. Båth M, Månsson LG. Visual grading characteristics (VGC) analysis: A non-parametric rank-invariant statistical method for image quality evaluation. *Br J Radiol* 2007, Mar;80(951):169-76.
15. Carmichael, Macca JA, Moores, Schibilla, Teunen, Van Tiggelen, Wall. European guidelines on quality criteria for diagnostic radiographic images. Brussels: ECSC-ES-EAEC; 1996.
16. Pascoal A, Lawinski CP, Honey I, Blake P. Evaluation of a software package for automated quality assessment of contrast detail images--comparison with subjective visual assessment. *Phys Med Biol* 2005, Dec 7;50(23):5743-57.
17. Marsh DM, Malone JF. Methods and materials for the measurement of subjective and objective measurements of image quality. *Radiat Prot Dosimetry* 2001;94(1-2):37.
18. Körner M, Treitl M, Schaetzing R, Pfeifer KJ, Reiser M, Wirth S. Depiction of low-contrast detail in digital radiography: Comparison of powder- and needle-structured storage phosphor systems. *Invest Radiol* 2006, Jul;41(7):593-9.
19. Börjesson, Hakansson, Bath. A software tool for increased efficiency in observer performance studies in radiology. *Radiat Prot Dosimetry* 2005;114(1-3):45-52.
20. Håkansson M, Svensson S, Zachrisson S, Svalkvist A, Båth M, Månsson LG. VIEWDEX: An efficient and easy-to-use software for observer performance studies. *Radiat Prot Dosimetry* 2010;139(1-3):42-51.
21. Bontrager KL, Lampignano JP. Radiographic positioning and related anatomy workbook and laboratory manual. Vol. 1, chapters 1-13. St. Louis; London: Elsevier Mosby; 2005.
22. Clark KCPIR. Clark's positioning in radiography. London: Hodder Arnold ; New York, NY : Distributed in the U.S. of America by Oxford University Press; 2005.
23. McQuillen-Martensen K. Radiographic image analysis. St. Louis, Mo.: Elsevier Saunders; 2006.
24. Gruber M, Weber M, Homolka P, Nemeš S, Fruehwald-Pallamar J, Uffmann M. Feasibility of dose reduction using needle-structured image plates versus powder-structured plates for computed radiography of the knee. *AJR Am J Roentgenol* 2011, Aug;197(2):W318-23.

25. Tsalafoutas IA, Blastaris GA, Moutsatsos AS, Chios PS, Efstathopoulos EP. Correlation of image quality with exposure index and processing protocol in a computed radiography system. *Radiat Prot Dosimetry* 2008;130(2):162-71.
26. Samei E, Badano A, Chakraborty D, Compton K, Cornelius C, Corrigan K, et al. Assessment of display performance for medical imaging systems: Executive summary of AAPM TG18 report. *Med Phys* 2005;32:1205.
27. Tingberg A, Sjöström D. Optimisation of image plate radiography with respect to tube voltage. *Radiat Prot Dosimetry* 2005;114(1-3):286-93.
28. IPEM. Measurement of the performance characteristics of diagnostic x-ray systems : Digital imaging systems. York: Institute of Physics and Engineering in Medicine; 2010.
29. Borasia G, Samei E, Bertolini M, Nitrosi A, Tassoni D. Contrast-detail analysis of three flat panel detectors for digital radiography. *Med Phys* 2006, Jun;33(6):1707-19.
30. Willis CE. Strategies for dose reduction in ordinary radiographic examinations using CR and DR. *Pediatr Radiol* 2004, Oct;34 Suppl 3:S196

Personal Information